Accepted Manuscript online: 2022-09-29 Article published online: 2022-10-28

Temperature-Dependent Dual Fluorescence from Small Organic Molecules

Min Wang[a]
Run-Ze Wang[a]
Cui-Hua Zhao* [a]

[a] School of Chemistry and Chemical Engineering, Shandong University, Shanda Nanlu 27, Jinan 250100, P. R. of China

* chzhao@sdu.edu.cn

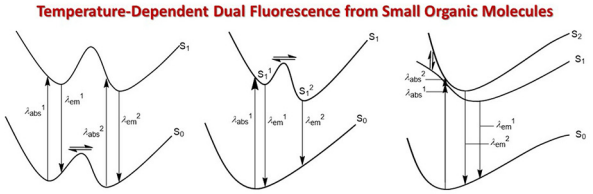

Received: 25.07.2022
Accepted after revision: 21.09.2022
DOI: 10.1055/a-1953-0322; Art ID: OM-2022-07-0027-SR

Abstract The temperature-dependent dual fluorescence from a single component of small organic molecules (SOMs) is very promising for the ratiometric fluorescence sensing of temperature. However, the SOM-based fluorophores typically only show one fluorescence band. It is thus very challenging to achieve dual fluorescence, let alone the dual fluorescence that is sensitive to temperature. Herein, in this short review, we briefly summarized the examples of SOM-based fluorophores exhibiting temperature-dependent dual fluorescence. Through representative examples, we mainly focus on the illustration of the intrinsic mechanisms of this unusual phenomenon, which may take place because of the presence of two local minimum conformations that are thermally equilibrated in the ground state, the presence of two local minimum conformations in the first excited state as the result of significant structural relaxation upon excitation, or the presence of thermal equilibrium between the first and second excited states. Hopefully, the discussions in this short review will provide some important guidelines for the further rational molecular design of such fluorophores.

Key words: small organic molecules, temperature-dependent dual fluorescence, local minimum conformations, ground state, excited state, thermal equilibrium

Introduction

Temperature is a crucial physical parameter in a wide range of fields such as biology, chemistry, industry and even our daily life. Therefore, the development of thermometric methods to detect variations of temperature is particularly important not only for scientific research but also for technological development.[1] Among the various temperature-determining methods developed so far, the fluorescence-based sensing methods are most promising due to their unique advantages, such as noninvasiveness, fast response, high spatial resolution, and capability of real-time monitoring.[2] According to the output signals, the thermo-responsive fluorescent systems can be typically classified into two categories. One relies on the absolute-intensity change of a single emission and the other takes advantage of change in the intensity ratio of two emission bands. The temperature sensing based on the single-emission intensity easily suffers from errors caused by the fluorophore concentration, the power of the excitation laser, the inhomogeneous distribution of the fluorophore, and the sensitivity of the detector. In contrast, the ratiometric sensing mode by measuring the change in the intensity change of two emission bands can overcome the above undesired effects. It is thus highly desirable to achieve temperature-dependent dual fluorescence.

To achieve the fluorescence ratiometric sensing of temperature, two approaches are generally adopted. One is to refer the signal of indicator to that of a temperature-insensitive fluorophore. The other is to utilize the dual emission of a single component. From the practical point of view, the latter method is more attractive because it can avoid the extra calibration due to the different physiochemical properties between two different components. The hereto reported fluorophores for the ratiometric fluorescence sensing of temperature mainly focus on hybrid nanoparticles,[3] polymers[4] and rare-earth complexes,[5] which either require complicated fabrication processes or are unstable in polar solvents and easily quenched by oxygen. In this context, the small organic molecule (SOM) fluorophores of a single component can provide good solutions to these problems.[6] However, the design of such fluorophores is a very challenging issue. According to the Kasha's rule, which states that "regardless of which electronic state of a given multiplicity is excited, the emitting electronic level of a given multiplicity is the lowest excited level of that multiplicity,"[7] the single-component SOM-based fluorophores generally display only one fluorescence band from the lowest singlet excited state (S_1). As a consequence, dual fluorescence is an abnormal photophysical phenomenon, let alone the dual fluorescence that is sensitive to temperature.

Biosketches

Ms. Min Wang received her B.S. degree from Qingdao University of Science and Technology in 2018, and M.S. degree from Shandong University in 2021, under the supervision of Prof. Hongyin Gao. Currently, she is a second-year Ph.D. candidate working in School of Chemistry and Chemical Engineering in Shandong University, under the supervision of Prof. Cui-Hua Zhao. She is interested in emissive small organic molecules based on chiral triarylboranes.

Mr. Run-Ze Wang received B.S. and M.S. degrees from Qingdao University of Science and Technology under the supervision of Prof. Shanfeng Xue in 2019 and 2022, respectively, working on blue organic light-emitting diodes (OLEDs). Now he is a first-year Ph.D. candidate working on chiral triarylborane-based emissive small organic molecules, under the supervision of Prof. Cui-Hua Zhao in Shandong University.

Cui-Hua Zhao is currently a full professor of Organic Chemistry in Shandong University. She received her Ph.D. degree in Organic Chemistry from Institute of Chemistry, Chinese Academy of Sciences in 2004, under the supervision of Prof. Dong Wang and Prof. Yong-Jun Chen. From 2004 to 2007, she worked in Prof. Shigehiro Yamaguchi's group in Nagoya University as a postdoctoral researcher with the support of the postdoctoral fellowship from Japan Society for the Promotion of Science (JSPS). In 2007, she joined the School of Chemistry and Chemical Engineering of Shandong University as an associate professor to start independent research. Her research interest mainly focuses on the design, synthesis, properties, and applications of emissive small organic molecules.

Theoretically, the prerequisite for the temperature-dependent dual fluorescence from a single-component SOM is the presence of two emissive species, which may be chemically isomeric or conformationally isomeric. Here we are mainly interested in the latter situation. In addition, the population of two emissive species is sensitive to temperature. The careful examination on the reported examples of temperature-dependent dual fluorescence of SOMs found that the presence of two emissive species may be caused by the presence of two local minimum conformations in the ground state (S_0) that interchange with each other,[8–10] the presence of two local minimum conformations in the S_1 state originating from significant conformational relaxation upon excitation,[11–14] and the presence of thermal equilibrium between S_1 and the second excited state (S_2)[15–18] (Figure 1). Considering the great potential utilization of SOM fluorophores showing temperature-dependent dual fluorescence for the ratiometric fluorescence sensing of temperature and the significant difficulty to obtain such fluorophores, we would like to present a short review on the existing samples. Especially, the analysis of the intrinsic mechanism behind experimental phenomena is significantly important. Herein, we mainly focus on the illustration of the three mechanisms through introduction of representative examples. Hopefully, the discussions in this short review will provide some important guidelines for the new design of such fluorophores.

Presence of Two Local Minimum Conformations in the S_0 State

For most fluorescent SOMs, there exists only one local minimum conformation in the S_0 state, which thus corresponds to the global minimum conformation in the S_0 state. Upon excitation, this conformation relaxes to the global minimum conformation of the S_1 state and emits fluorescence. In some circumstances, one local minimum conformation may surpass a certain energy barrier and transform to another one in the S_0 state. Namely, there exist two local minimum con-

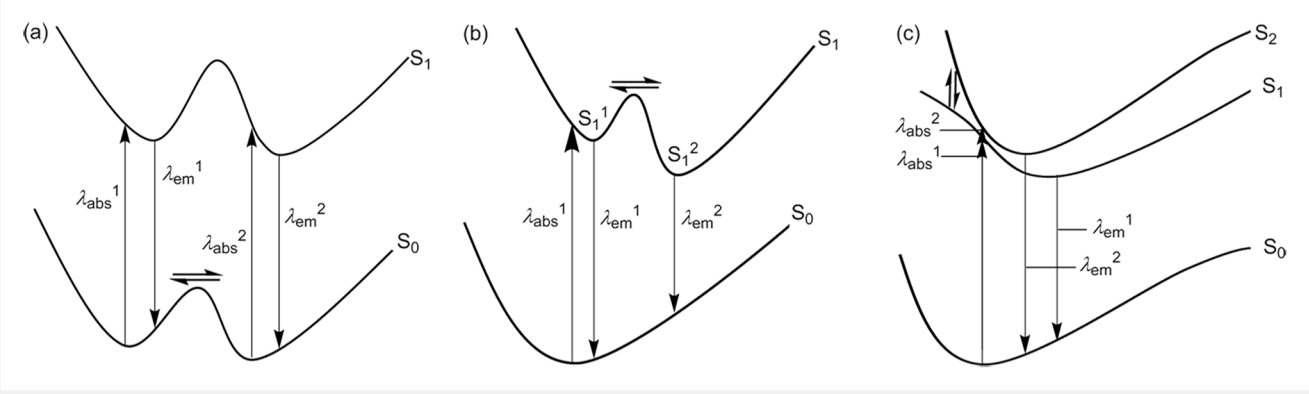

Figure 1 Schematic presentations for the mechanisms of temperature-dependent dual fluorescence, which arise from the presence of (a) two local minimum conformations in the S_0 state, (b) two conformers in the S_1 state originating from significant conformational relaxation upon excitation, and (c) the thermal equilibrium between S_1 and S_2 states.

formations that are thermally equilibrated in the S_0 state (Figure 1a). In addition, the two stable conformers may display different electronic structures and thus different absorption and fluorescence properties due to their different stereostructures. Owing to the thermal equilibrium, the population of each local minimum conformation is sensitive to temperature. The increase of temperature is expected to increase the population of the local minimum conformation with relatively higher energy. Therefore, the individual excitation of both conformers will give rise to temperature-dependent dual fluorescence. The change trend of fluorescence as temperature varies is expected to be closely related to the relative stability and the emission properties of each conformer. Due to different absorption and emission properties of two conformational structures, both fluorescence and absorption change with the change in temperature. So far, it has been very difficult to predict which conformer is more stable. In addition, the more stable conformer in the S_0 state does not necessarily show a higher stability in the S_1 state, which makes it very hard to compare two emission wavelengths and the change trend of fluorescence.

Triarylboranes represent good examples to illustrate this mechanism. Owing to the Lewis acidity of the trivalent boron center, it can accept electrons from Lewis basic donors, such as N, P, or O, to form reversible B–X bond coordination bonds. By finely tuning the intramolecular relative positions and steric hindrance between boron and Lewis basic donors, it becomes possible to modulate the B–X bond strength to achieve the reversible transformation between three-coordinated and four-coordinated species,[8–10,19] which may be stimulated by temperature. One pioneering system possessing switchable B–X bonds is the bithiophene Lewis pair **1** (Figure 2),[8] in which diphenylphosphine oxide $P(O)Ph_2$ and dimesitylboryl ($BMes_2$) were introduced at 3,3′-poistions of 2,2′-bithiophene. One important structural feature of **1** is the flexibility of the bithiophene backbone, which allows

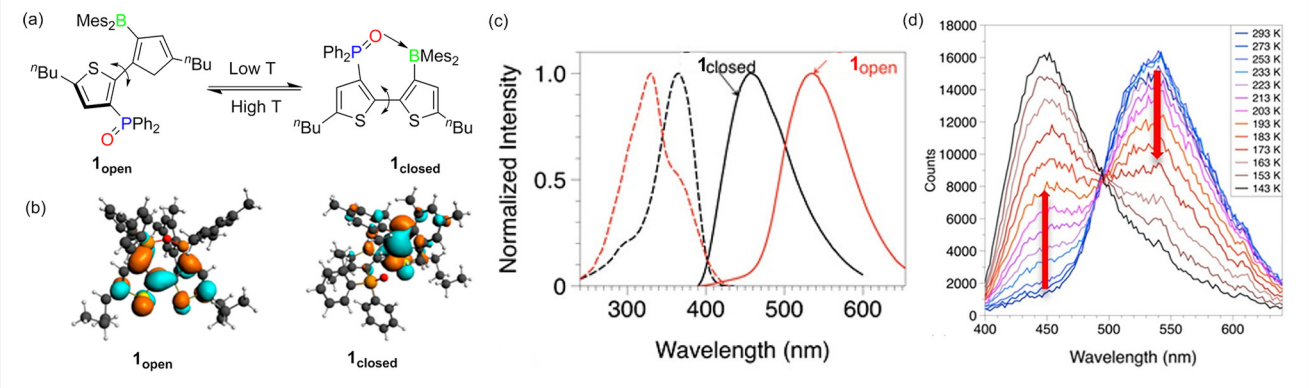

Figure 2 (a) Chemical structure of **1** and its intramolecular thermochromic B–O switching. (b) LUMO diagrams of **1**. (c) Normalized emission and excitation spectra of $\mathbf{1}_{closed}$ in hexane (black trance) and $\mathbf{1}_{open}$ in methanol (red trace). (d) Emission spectra of **1** in MeOH/EtOH (v/v = 1 : 4) at variable temperatures. Adapted with permission from Ref. 8a. Copyright 2015 American Chemical Society.

for interannular C–C bond rotation, leading to the flexible switching between the closed form as a Lewis adduct and the open form as an unbound Lewis pair. In addition, the flexible switching of **1** between two different forms is greatly influenced by the H-bonding capability of the solvent, which was strongly supported by the IR and NMR spectra. In weak or non-H-bonding donor solvents, such as hexane, the closed forms are present. However, the open form is favored in a strong H-bonding solvent, such as MeOH, and two structures coexist in weak H-bond-donating solvents like CH_2Cl_2. It is well known that tri-coordinated boron exhibits strong electron-accepting ability. The formation of the B–O bond in **1** between the B center and the O atom of P=O resulted in the great difference in the electronic structures and thus different absorption and emission properties between the open and closed forms. Theoretical calculations demonstrate the $S_0 \rightarrow S_1$ transition of the open form is characterized by a charge-transfer (CT) process from a mesityl-localized π-orbital to boron-centered LUMO due to the electron-accepting ability of $BMes_2$.[20] In contrast, the $S_0 \rightarrow S_1$ excitation of the closed form features a bithiophene π–π* transition along with a CT from a mesityl π-orbital to the bithiophene-localized LUMO. Consistent with the solvent dependence of flexible switching between the open and closed forms of **1**, both the absorption and emission are sensitive to the solvent. In very weak or non-H-bonding donor solvents, such as hexane, the spectra show a dominant band at ≈ 370 nm. However, this band becomes weaker and the bands between 260 and 350 nm become stronger with increasing H-bonding ability. Regarding the emission, this compound shows bright greenish yellow fluorescence ($\Phi_F = 0.60$) at 540 nm in methanol and emits a bright blue emission at 440 nm in hexane, which correspond to the open and closed forms, respectively (Figure 2c). Moreover, the emission of **1** in alcohol is highly temperature-dependent. At room temperature, where the open form is the major species, the emission is dominated by the fluorescence at ≈ 540 nm. As the temperature decreases, the initially dominant band at 540 nm decreases with a concomitant increase in the emission band at 440 nm, suggesting lowering the temperature is favorable for the formation of the closed form. The temperature dependence of the equilibrium between the two forms of **1** is reasonably explained by their entropy difference. Comparatively, the closed form has a lower entropy due to the increased rigidity. It was noted that the structure of phosphine oxide plays an important role in the flexible switching between Lewis adducts and unbound Lewis pairs. The analogous compound containing di(*i*-propyl) phosphine oxide behaves similarly to **1** and the analogue with dimesityl phosphine oxide always exists as the unbound Lewis pairs of the open form. This may be due to that the B–O bond strength is greatly affected by electronic and steric effects of the substituent on the phosphor atom.

Another more recent example of triarylborane with switchable B–O bond and temperature-dependent dual fluorescence is an *ortho*-$BMes_2$-substituted benzaldehyde derivative **2**,[9] in which the B–O bond is formed between the B center and the O atom of C=O instead of P=O. It was well established by NMR experiments that this compound exists as the open form in various solvents. Upon addition of water to the THF solution of **2**, the B–O bond formation is favored to form the Lewis adduct, probably due to the possible interaction of water with the amino group, which would reduce the electron-donating ability of the amino group to the boron center and thus enhance the electrophilicity of the boron center to facilitate the B–O bond formation. Again, this molecule emits distinct fluorescence in its two different forms. In THF, where **2** exists solely as the open form; a bluish green fluorescence at 490 nm ($\Phi = 0.61$) was observed. This fluorescence is typical of a CT transition. After the water content reaches 70%, where the closed form is dominant, the solution ultimately gives orange-red fluorescence at a much longer wavelength ($\lambda_{em} = 605$ nm; $\Phi = 0.02$). Moreover, the switching between the open and closed forms of **2** is also responsive to temperature, which was only observed below the melting points of the solvent (m. p. = 205 K for 2-methoxyethyl ether [MOE] and 176 K for CH_2Cl_2). From the temperature of m. p. to 77 K, a decrease in temperature facilitates the switching from the open form to the closed form, causing the decrease of shorter wavelength fluorescence band and a simultaneous increase of longer wavelength fluorescence band. This change trend of fluorescence with varying temperature is similar to **1**. Above the m. p., the fluorescence is gradually blue-shifted with increased intensity as temperature increases, which is ascribed to the CT character for the emission in the open form. If the aldehyde group is replaced by a methyl ketone group, the corresponding analogue exists only in its closed form due to the stronger nucleophilicity of ketone as the result of the electron-donating ability of methyl. In contrast to the full characterization of fluorescence at various temperatures, the influence of temperature on the absorption was not examined for **1** and **2**. However, structural analysis through the NMR technique undoubtedly proved the reversible conversion between the open and closed forms in the S_0 state for these two compounds.

In addition to the B–O bond, the switchable B–N bond has also been utilized to design stimuli-responsive triarylboranes. Similar to the triarylboranes with switchable B–O bond, an increase in temperature usually leads to the cleavage of B–N bond, giving rise to the temperature dependence of fluorescence. However, examples of such triarylboranes showing dual fluorescence are very limited because one of two species is probably nonemissive. One example of triarylborane with switchable B–N bond and temperature-dependent dual fluorescence is the diborylated bis(thienyl)-benzothiadiazole derivative **3** (Figure 3).[10] Although the in-

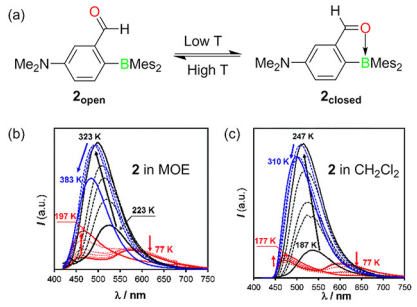

Figure 3 (a) Chemical structure of **2** and its intramolecular thermochromic B–O switching. (b) Emission spectra of **2** in MOE at various temperatures. (c) Emission spectra of **2** in CH_2Cl_2 at various temperatures. Adapted with permission from Ref. 9. Copyright 2018 Royal Society of Chemistry.

tramolecular B–N bond of this compound is absent in the X-ray crystal, the mono-closed form exists to some extent in solution. According to the density functional theory (DFT) calculations, the Gibbs free energy between the open and mono-closed forms is small ($\Delta G = 1.02\ kcal \cdot mol^{-1}$), which supports the possible formation of both isomers and an easy transformation between them. Moreover, the ratio of the mono-closed form increases with decreasing temperature. This was supported by the temperature-dependent absorption spectra, in which the bands at 575 and 422 nm were assigned to the absorption of the open and closed forms, respectively. Based on the analysis of the absorbance by using the oscillator strengths obtained from time-dependent DFT (TD-DFT) calculations, the abundance ratio of the open and mono-closed forms in toluene was estimated to be 85 : 15 at 100 °C, 47 : 53 at 20 °C, and 9 : 91 at −40 °C. Along with facile transformation between the open and mono-closed forms, the fluorescence is sensitive to temperature (Figure 4).[10] In toluene solution, the two fluorescence bands corresponding to the open and closed forms are located at 568 nm ($\Phi_F = 0.12$, $\lambda_{ex} = 470$ nm) and 718 nm ($\Phi_F = 0.02$, $\lambda_{ex} = 590$ nm), respectively. Upon cooling, the orange-yellow band at ≈ 560 nm gradually decreases and almost disappears at −40 °C. On the contrary, the near-infrared fluorescence band at ≈ 720 nm is increased. It was noted that the two different forms of **3** have to be excited with different wavelengths due to the significant difference of their absorption. This still provides a good example to achieve temperature-dependent dual fluorescence by utilizing the switchable B–N bond. Clearly, utilization of the switchable B–X (B–O/B–N) bond is an efficient strategy for the design of SOMs showing temperature-dependent dual fluorescence. It seems the response temperature range is highly influenced by the B–X bond strength. It is still a very tricky problem to control the B–X bond strength and to tune the response temperature range.

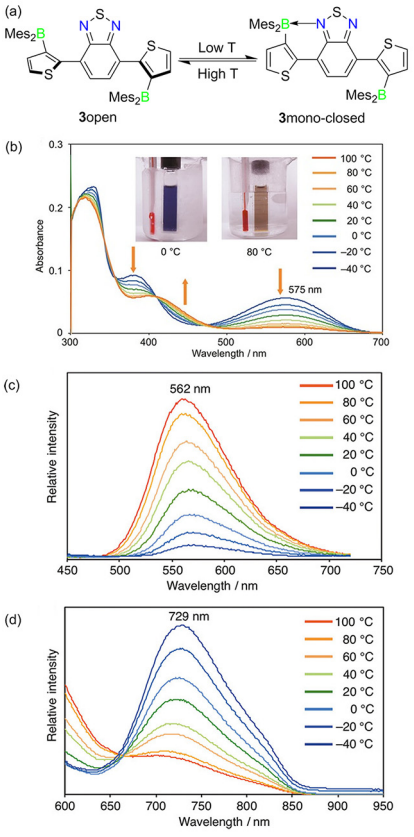

Figure 4 (a) Chemical structure of **3** and its intramolecular thermochromic B–N switching. (b) Thermochromism of **3** in toluene. The wavelength of the longest absorption bands and photographs of solutions are included. Temperature-dependent fluorescence spectra of **3** in toluene when excited at (c) 370 nm and (d) 540 nm. Adapted with permission from Ref. 10. Copyright 2017 Wiley-VCH.

Presence of Two Local Minimum Conformations in the S_1 State

Generally, the fluorescence arises from the initial minimum conformation in the S_1 state, which is also the global minimum and is reached through structural relaxation upon excitation from the S_0 state. From the initial minimum (S_1^1), if the fluorophore overcomes a certain energy barrier and can reach another more stabilized local minimum (S_1^2) through much more significant structural relaxation, the dual fluorescence from both local minima may be observed (Figure 1b). In this situation, the initial minimum (S_1^1) usually emits at the shorter wavelength. The increase in temperature would facilitate the transformation from S_1^1 to S_1^2, leading to the increasing fluorescence intensity ratio of the longer wavelength band. Since both fluorescence bands originate from the S_1 state, the Kasha's rule still works. In ad-

dition, the absorption is independent of the temperature since two emission bands arise from the S_1 state.

One typical example of SOMs that show temperature-dependent dual fluorescence following this mechanism is a class of *N,N'*-disubstituted-dihydrophenazine derivatives,[11] which were reported by Tian and coworkers. Among them, the *N,N'*-diphenyl (**DPAC**) and *N*-phenyl-*N'*-fluorenyl (**FIPAC**) dihydrophenazines are two representative compounds (Figure 5). In the S_0 state, they adopted a nonplanar distorted structure for the dihydrophenazine framework as a result of steric hindrance between the *N,N'*-disubstituents and phenanthrene ring. Upon excitation, the initial CT S_1 state with saddle-shaped non-planar structure for the dihydrophenazine moiety emits blue fluorescence due to the limited overall conjugation. In the electronically excited S_1 state, the molecule easily undergoes bent-to-planar vibration and finally reaches a planarized S_1 state, which emits red fluorescence as a result of an elongated conjugation. This phenomenon was coined as vibration-induced emission (VIE).[12] Since the intramolecular vibration is greatly dependent on rigidity of the surrounding environment, which is sensitive to temperature and viscosity, the emission can be tuned by modulation of the intramolecular vibrations through changing the temperature. Therefore, these two compounds show temperature-dependent fluorescence. For the solution of **FIPAC** in *n*-butanol, the temperature dependence of fluorescence was mainly observed within the temperature range of 133 – 233 K (−140 to −40 °C). At 133 K, this compound only shows the blue emission at 425 nm, which corresponds to the deactivation of the intrinsically saddle-shaped structure of the S_1 state. As the temperature increases, this band decreases gradually with concomitant emergence of a red fluorescence band, which becomes dominant and is maximized at 610 nm at 233 K. Such a change in fluorescence was ascribed to the more facile skeletal motion toward the planarization with increasing temperature and thus minimizing rigidity of the surrounding environment. Similar temperature-dependent fluorescence was also observed for **DPAC** within the temperature range of 133 – 193 K (−140 to −80 °C) and it emits blue fluorescence and orange-red fluorescence at 133 and 193 K, respectively. For the solution of the above two compounds, the fluorescence response to temperature is only limited to a relatively narrow temperature range. In addition, a very low temperature is required to trigger the fluorescence response. This may be caused by the small energy barrier for the geometry transformation of dihydrophenazine. In contrast, the required temperature to trigger the fluorescence response of a solid sample is too high due to a very large energy barrier. The relatively narrow temperature scope and the too high/too low temperature for the fluorescence response restrict their practical applications. In order to modify the temperature sensing range to a suitable scope, Mei and coworkers designed three fluidic dihydrophenazine dyes, **DPC, DPSi-1**, and **DPSi-2**, by attaching flexible side alkyl/siloxane chains onto the dihydrophenazine core (Figure 6).[13] Compared with the solid sample, the reduced intermolecular interactions of the pure fluidic substance will lower the energy barrier of conformation transformation in the electronically excited S_1 state and thus tune the dynamic range of fluorescence temperature sensing to a suitable range. It was well demonstrated that all these three dihydrophenazine derivatives can serve as excellent ratiometric fluorescence thermometers with high sensitivity, a broad temperature range (5 – 135 °C) and fairly good reversibility. For example, **DPSi-1** exhibits linear response within the temperature range of 50 – 135 °C with sensitivity up to 3.40% per °C at 135 °C. Moreover, the fluorescence color changes from blue to greenish-blue and near-white and finally to orange-red with increasing temperature, which is easily detected by the naked eyes.

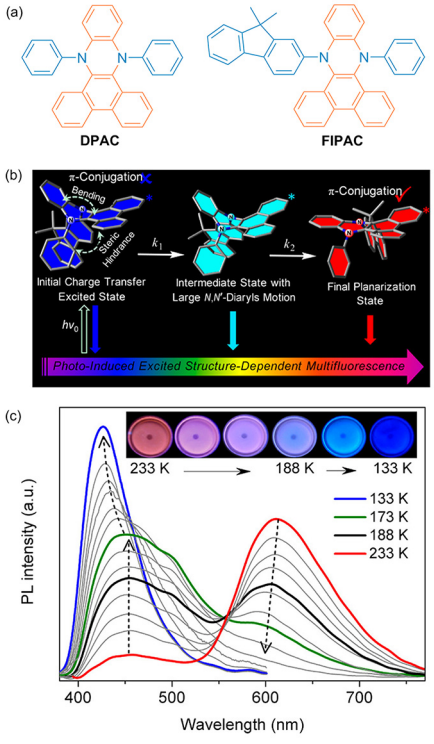

Figure 5 (a) Chemical structures of *N,N'*-disubstituted-dihydrophenazine **DPAC** and **FIPAC**. (b) Emission mechanism for the multifluorescence of **FIPAC**. (c) Temperature-dependent fluorescence spectra of **FIPAC** in *n*-butanol from 233 to 133 K with various viscosities. The arrows indicate the direction of fluorescence response upon reducing the temperature. Inset: photographs under 365 nm UV light. Adapted with permission from Ref. 11. Copyright 2015 American Chemical Society.

In addition to *N,N'*-disubstituted-dihydrophenazine derivatives, another representative example of SOMs showing temperature-dependent dual fluorescence as a result of the

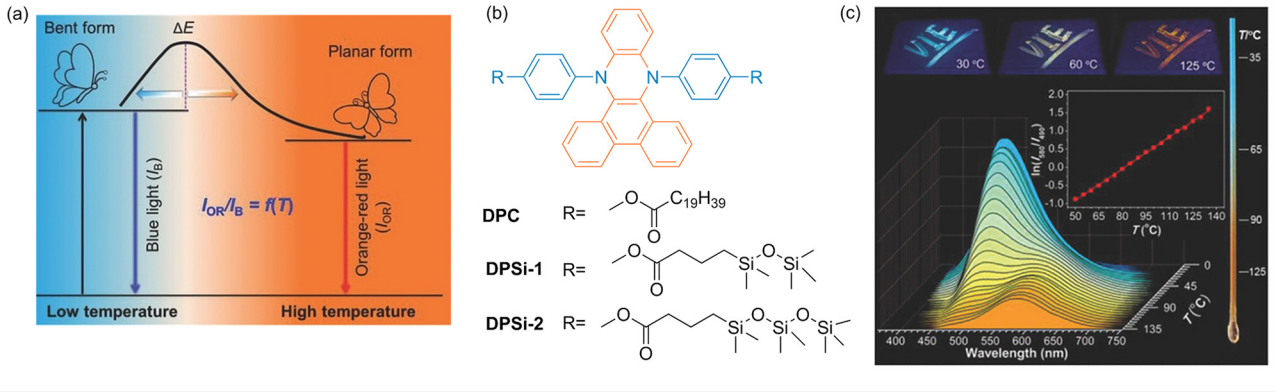

Figure 6 (a) Schematic illustration of the working principle of the ratiometric thermometers constructed based on the VIE mechanism. (b) Chemical structure of AIE-active *N,N'*-diphenyl dihydrophenazines, **DPC, DPSi-1** and **DPSi-2**. (c) Emission spectra of **DPSi-1** noumenon recorded when the temperature was increased from 5 to 135 °C. Inset: The fitted plot of $\ln(I_{580}/I_{490})$ versus *T*, photograph of a melting-point tube filled with **DPSi-1** under illumination of UV light at 365 nm when it was subjected to site-reliable thermal treatment, and fluorescence photographs of **DPSi-1** scribbled on a ceramic heater at different temperatures. Adapted with permission from Ref. 13. Copyright 2018 Wiley-VCH.

dynamic conformational change in the excited state is the cyclooctatetraene (COT) derivative **4** (Figure 7),[14] which was reported by Yamaguchi and coworkers. This compound consists of a flexible COT core unit and two emissive rigid rings of anthraceneimide. At room temperature, the CH_2Cl_2 solution of **4** displays green fluorescence with the maximum wavelength located at 520 nm together with vibronic peaks at 561 and 611 nm as well as a weak shoulder band in a higher energy region around 460 nm. The fluorescence spectrum in 2-methyltetrahydrofuran (MTHF) solution is very close to that in CH_2Cl_2. Importantly, this compound shows a dramatic emission change between a green fluorescence and a blue fluorescence with decreasing temperature and thus with increasing viscosity of MTHF. From 296 to 163 K, the green fluorescence of **4** is only gradually increased in intensity without any significant shifts in energy, which results from the retarded nonradiative decay process at lower temperature. However, the further decrease of temperature led to the decrease of intensity for the green fluorescence covering 500 – 650 nm and a concomitant increase of the blue fluorescence shoulder band in the shorter wavelength region from 420 to 500 nm. At 133 K, the intensities of the two bands are comparable to each other. At 77 K, compound **4** finally shows the sole blue fluorescence at 433 nm with vibronic peaks at 460 and 491 nm. In contrast to the remarkable temperature dependence of fluorescence, no temperature dependence was observed for the excitation spectra from 296 to 77 K, regardless of the emission wavelengths. Theoretical calculations for the model compound **4′** demonstrated that the most stable geometry (the global minimum) in the S_1 state is a planar conformation, for which the bent angle (θ) of COT is 0°, while the V-shaped structure ($\theta = 40.6°$) is most stable in the S_0 state. In addition, **4′** also has a local minimum at $\theta = 22.8°$. Herein, the temperature-dependent dual fluorescence for **4** was well explained by the conformational transformation of the COT core unit from the V-shaped structure to the planar structure in S_1, which gave the blue and green fluorescence, respectively. At lower temperatures, the conformational change in the S_1 state is more restricted, leading to a decreased intensity of the green fluorescence and an increased intensity of the blue fluorescence. Probably due to the very small energy barrier for the conformational change, the temperature-dependent dual fluorescence was only observed below 163 K. When the temperature is higher than 163 K, the temperature change only leads to a change in the fluorescence intensity. The observation of blue fluorescence in solution at room temperature was explained by the small energy difference between the V-shaped and planar conformers in the S_1 state, as a result of which the V-shaped conformer exists with a certain percentage (7.69 % at 296 K). Although the authors did not explore the utility of compound **4** for ratiometric temperature fluorescence sensing, it definitely provides a good example for the temperature-dependent dual fluorescence and suggests that the combination of an emissive rigid skeleton with a COT core is an effective strategy to achieve this unusual property.

Presence of Thermal Equilibrium between S_1 and S_2 States

Although most fluorescent SOMs obey Kasha's rule and only show one fluorescence band from the S_1 state, the anti-Kasha fluorescence from the upper excited states, generally the S_2 state, is possible under some circumstances. Two prototype mechanisms are usually responsible for the anti-Kasha fluorescence from the S_2 state.[21] One is that the $S_0 \rightarrow S_2$

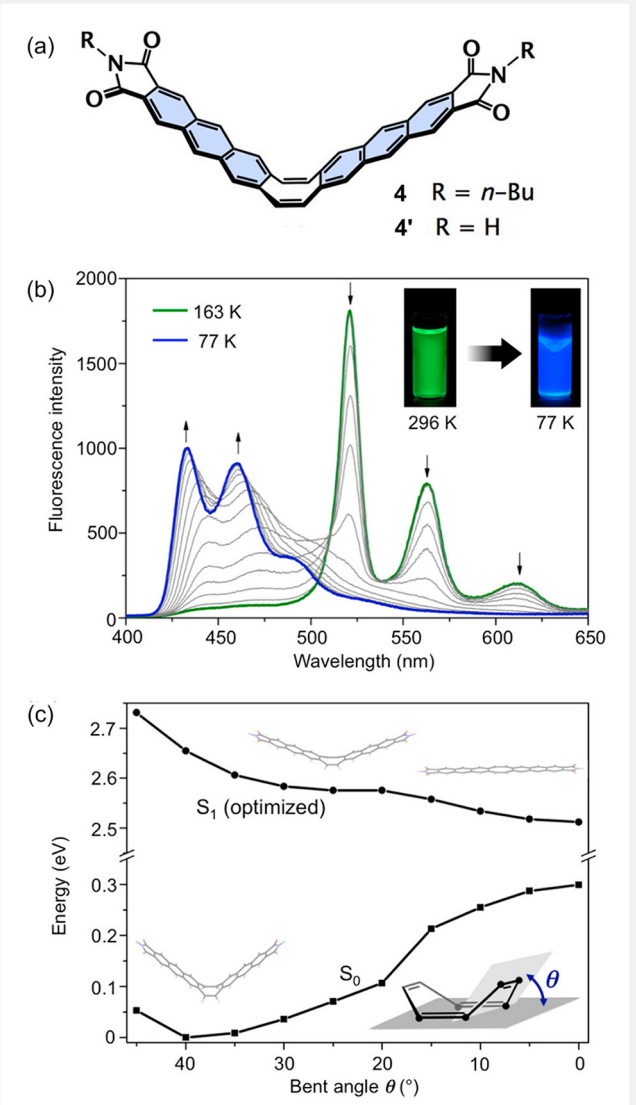

Figure 7 (a) Chemical structure of cyclooctatetraene derivatives. (b) Temperature-dependent fluorescence spectra of **4** in Me-THF from 163 K (solution) to 77 K (glass). λ_{ex} = 350 nm. (c) Calculated potential energy diagram for the S_0 and S_1 states of **4′** with fixed bent angle θ. The constrained geometry optimization was performed in the S_1 state at the PBE0/des-SV(P) level. Adapted with permission from Ref. 14a. Copyright 2013 American Chemical Society.

transition's possibility is large and the S_1–S_2 energy gap is large, which retards the internal conversion from S_2 to S_1. The other is that the S_1–S_2 energy gap is small, which enables the thermal population of S_2 from S_1. For the first case, the relative intensity of two fluorescence bands mainly depends on the rate of radiative and non-radiative decay processes from each excited state and thus basically is not affected by temperature. On the contrary, the high temperature would populate the S_2 state and thus increase the intensity ratio of shorter wavelength to longer wavelength when the thermal equilibrium between S_1 and S_2 exists due to the small energy gap (Figure 1c).

The SOMs with electron donor (D) and electron acceptor (A) units connected through π-linkers usually exhibit an intramolecular CT excited state, which is formed via the geometric rearrangement (planarization or twisting at the bridge between donor and acceptor units) following excitation to the locally excited (LE) state or by direct excitation from the S_1 state.[22] As the CT emission is highly sensitive to the surrounding environments, such as the solvent polarity, viscosity and temperature of the medium, such fluorophores are promising for the design of fluorescent sensors.[23] In addition to the CT emission, the emission from the LE state can also be detected sometimes. The thermal population of the LE state from the CT state might enable the ratiometric temperature sensing. One example of such fluorophores is the T-shaped pyridoquinoxaline derivative **PQCz-T** (Figure 8a),[15] in which two electron-donating carbazole groups were introduced at 2,7-positions. Theoretical calculations suggest that the $S_0 \rightarrow S_1$ excitation of **PQCz-T** corresponds to the transition from the HOMO mainly located on the electron-donating carbazole units to the LUMO predominantly located on the π-electron-deficient central framework. The obvious HOMO–LUMO charge separation implies the facile D–A rotation and the twisted intramolecular CT (TICT) characteristics in the S_1 state, which was proved by the substantial fluorescence solvatochromism from 564 nm in toluene and 631 nm in dichloromethane. The HOMO and LUMO distributions for the optimized S_1 geometry, which are very similar to those of the optimized S_0 geometry, confirmed the CT character of the S_1 state. Notably, the fluorescence of **PQCz-T** in THF is very sensitive to temperature. As the temperature drops from room temperature (298 K) to 263 K, the yellow fluorescence at 580 nm is gradually red-shifted to 610 nm with an increased intensity. On the contrary, the emission is blue-shifted with the gradual increase in temperature. Especially, a new peak around 415 nm was observed at 338 K. The good linear relationship between the ratio of fluorescence intensities (415 and 610 nm) and temperature illustrated the promising utilization of this compound for the ratiometric fluorescence temperature sensing. The appearance of the blue-emitting fluorescence at 415 nm was explained by authors through the dynamic equilibrium between the LE and TICT states. Upon heating, the molecule with the intensified molecular motion is able to cross the thermal barrier between TICT and LE states and the preferential population of the LE state causes the blue shift of the fluorescence. However, the inherent feature of the LE state was not further investigated. Judging from the intramolecular charge transfer character of S_1, the LE state of **PQCz-T** is probably assigned to the S_2 state. A careful examination of the excitation spectra of this band and the theoretical composition of $S_0 \rightarrow S_2$ excitation using TD-DFT cal-

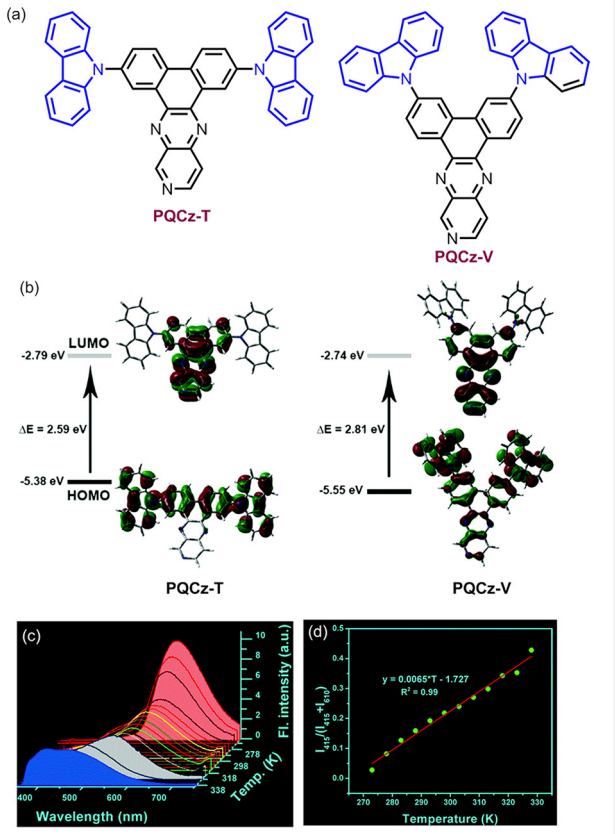

Figure 8 (a) Chemical structures of **PQCz-T** and **PQCz-V**. (b) The obtained ground state HOMO and LUMO distributions and the respective energy values of **PQCz-T** and **PQCz-V** obtained via DFT calculations at the B3LYP/6–31 G(d,p) level. (c) Fluorescence spectra of **PQCz-T** in THF from 263 to 338 K (λ_{ex} = 340 nm). (d) The plot of the ratio of fluorescence intensity $I_{415}/(I_{415} + I_{610})$ of **PQCz-T** versus *T*. Adapted with permission from Ref. 15. Copyright 2018 Royal Society of Chemistry.

culations based on the optimized S_0 geometry probably will provide a deeper insight into this point. The temperature-responsive emission property is very unique to **PQCz-T**. The temperature influence on the fluorescence is much less significant for its regioisomer **PQCz-V**, in which two carbazole groups were introduced at 3,6-positions. The HOMO of **PQCz-V** is delocalized over the whole molecule due to the more efficient conjugation from the donor to the acceptor, which would probably make the molecule more rigid and rules out the emergence of the temperature-dependent fluorescence behavior.

Through thermal population of the LE state from the TICT state, Yang and co-workers have developed a series of fluorescence temperature sensors based on triarylboranes (Figure 9),[16,24] which exhibit temperature-dependent dual fluorescence. The prototype compound is **DPTB**, in which the electron-deficient boron facilitates CT transitions in the

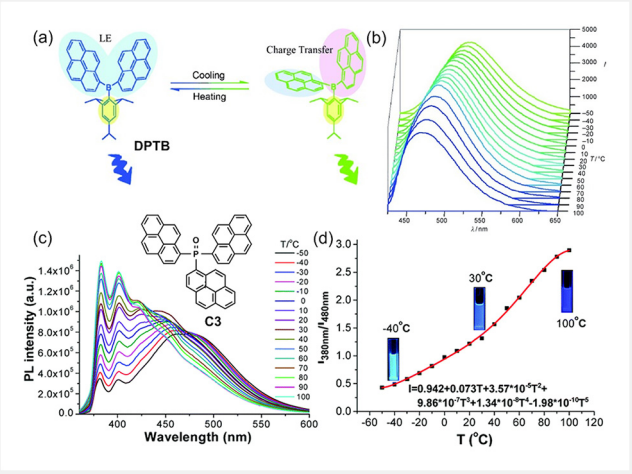

Figure 9 (a) Chemical structure of **DPTB** and the mechanism of its emission changes with temperature. (b) Corrected emission spectra of **DPTB** in MOE recorded between −50 and 100 °C (λ_{ex} = 410 nm). (c) Chemical structure and emission spectra of **C3** in MOE recorded from −50 to 100 °C (λ_{ex} = 360 nm). (d) Temperature dependence of the ratio of fluorescence intensity (I_{380}/I_{480}) of **C3**. Adapted with permission from Refs. 16 and 17. Copyright 2011 Wiley-VCH and 2017 Royal Society of Chemistry, respectively.

excited state. In addition, the contributions of the two pyrene units are not equivalent to each other in the excited state due to their different orientations around the boron atom. Although this compound displays only one fluorescence band at room temperature, the fluorescence decay dynamics suggested that this band is dual fluorescence. The shorter- and longer-wavelength bands are assigned to the emissions from the LE and TICT states, respectively. Owing to the merging of two emission bands, an increase in temperature from −50 to 100 °C (in MOE) is observed, causing consecutive hypsochromic shifts of fluorescence, and limiting its application as a ratiometric fluorescence thermometer. Following this design, Qian and co-workers designed tripyrenephosphine oxide **C3** to realize the ratiometric fluorescence measurement of temperature (Figure 9).[17] In polar solvents, this compound can show well-separated LE and CT emissions, which originate from the intra-pyrene π–π* transition and inter-pyrene CT. The fluorescence spectra of **C3** in MOE at various temperatures clearly demonstrate its utility as a ratiometric fluorescence thermometer. With the increase of temperature from −50 to 100 °C, the CT emission gradually decreases while the LE emission gradually increases. The plot of fluorescence intensity ratio between two emission bands versus temperature can be well fitted with a fifth-order polynomial with a correlation coefficient of 0.998. The temperature sensitivities (dI/dT) range from 0.012 °C^{-1} (−50 to 30 °C) to 0.024 °C^{-1} (30–100 °C). There is no doubt that the CT state of **DPTB** and **C3** corresponds to the S_1 state. However, whether the LE state corresponds to

the S_2 state or another conformation of the S_1 state has not been well clarified.

In 2019, our group disclosed a class of *o,o'*-substituted binaphthyl derivatives displaying temperature-dependent dual fluorescence (Figure 10),[18] which is well explained by the thermal equilibrium between S_1 and S_2. In the *o,o'*-substituted binaphthyl **BNMe$_2$-BNaph**, the electron-accepting dimesitylboryl ($BMes_2$) and the electron-donating *N,N*-dimethyl amino (NMe_2) were introduced to each naphthyl unit. Unlike the normal donor–π–acceptor (D–π–A), this compound essentially consists of two independent D–π–A subunits.[18a] It was found that this compound displays two well-separated fluorescence bands in polar solvents such as THF, MOE, and MeCN. In addition, the dual fluorescence of **BNMe$_2$-BNaph** is highly sensitive to temperature. In MOE, both emission bands (~478 nm and ~565 nm as shoulder peaks) become stronger with the shorter wavelength increasing more rapidly, which causes a significant increase of the fluorescence intensity ratio I_{478}/I_{565} from 0.29 to 4.95 and a remarkable fluorescence color change from yellow to blue. In addition, there is a good linear relationship between the fluorescence intensity ratio and temperature with the best sensitivity up to 4.7%/°C observed over a wide range of temperature from −20 to 80 °C, which indicates the great potential application of **BNMe$_2$-BNaph** as a ratiometric fluorescence thermometer. In conjunction with the experimental study and theoretical calculations, the dual fluorescence of **BNMe$_2$-BNaph** was assigned to the deactivation of S_1 and S_2, which have the inter-subunit CT character and the mixed intra-subunit CT and LE characters, respectively. The very similar calculated excitation energies of S_1 and S_2 (ΔE = 0.07 eV) suggest a thermal equilibrium, which explains the temperature-dependent dual fluorescence of **BNMe$_2$-BNaph**. The (NPh_2)-substituted analogue compound, **BNPh$_2$-BNaph**, provided essentially identical calculations. However, this compound shows only one fluorescence band in various solvents and the dual emission was observed only in the circularly polarized luminescence spectra, which may be explained by the close energies of the $S_1 \rightarrow S_0$ and $S_2 \rightarrow S_0$ deactivations and thus the merging of two emission bands. Moreover, the other *o,o'*-substituted binaphthyls, which also consist of two D–π–A subunits with $BMes_2$ replaced by CHO (**CHONMe$_2$-BNaph**) and CN (**CNNMe$_2$-BNaph**), respectively, also show temperature-dependent dual fluorescence with fluorescence changes in a similar manner to **BNMe$_2$-BNaph**,[18b] indicating the general utility of this molecular design for temperature-dependent dual fluorescence properties.

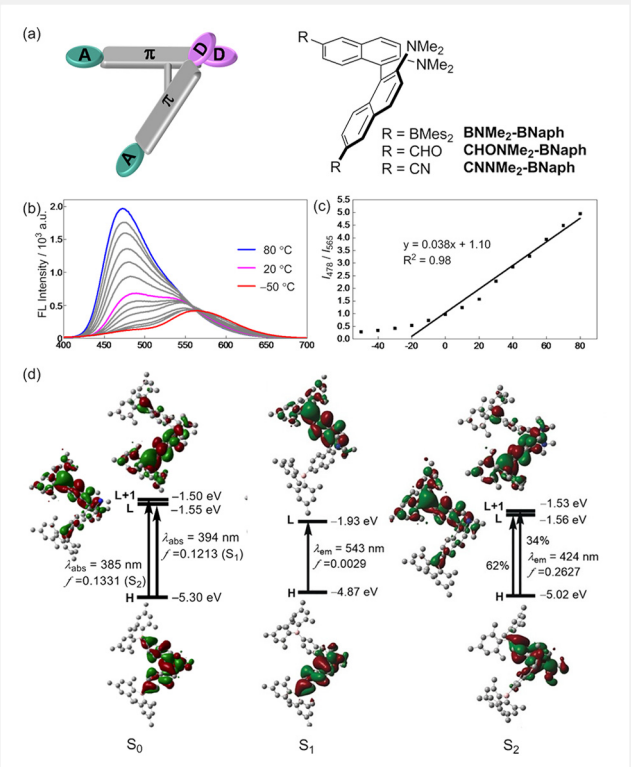

Figure 10 (a) Schematic presentation and structures of chemical structure of *o,o'*-substituted binaphthyls. (b) Fluorescence spectra and (c) fluorescence intensity ratios of the bands at 478 and 565 nm of **BNMe$_2$-BNaph** at various temperatures. (d) The Kohn–Sham energy levels, pictorial drawing of frontier orbitals, and transitions of **BNMe$_2$-BNaph** in the ground and excited states, calculated at TD/PBE0/6 – 31 G (d) levels.

Conclusions and Outlook

In summary, we have briefly summarized the examples of SOMs that show temperature-dependent dual fluorescence, which is a very unusual property but promising for the ratiometric fluorescence sensing of temperature. The examples provided here were included according to the inherent mechanism for the temperature-dependent dual fluorescence behavior, which may take place because of the presence of two local minimum conformations that are thermally equilibrated in the S_0 state, the presence of two local minimum conformations in the S_1 state as a result of significant structural relaxation upon excitation, and the presence of thermal equilibrium between S_1 and S_2 states. Ideally, the two fluorescence bands from a single SOM are intensive and well separated. As the temperature changes, one emission becomes stronger while the other becomes weaker, leading to a remarkable change in the fluorescence intensity ratio between the two emission bands. In addition, the temperature response of dual fluorescence occurs in the appropriate temperature range according to various environments. Despite some reported examples of SOMs showing temperature-dependent dual fluorescence, it is still very hard for

the rational molecular design to achieve the above performances. Hopefully, the discussion of the present examples, especially the inherent mechanism behind the experimental phenomena, will provide important basis for the design of new fluorophores that display temperature-dependent dual fluorescence with improved performances and their practical applications.

Funding Information

This work was supported by the National Natural Science Foundation of China (21971150).

Conflict of Interest

The authors declare no conflict of interest.

References

(1) (a) Mecklenbrug, M.; Hubbard, W. A.; White, E. R.; Dhall, R.; Cronin, S. B.; Aloni, S.; Regan, B. C. *Science* **2015**, *347*, 629. (b) Kucsko, G.; Maurer, P. C.; Yao, N. Y.; Kubo, M.; Noh, H. J.; Lo, P. K.; Park, H.; Lukin, M. D. *Nature* **2013**, *500*, 54. (c) Brites, C. D. S.; Lima, P. P.; Silva, N. J. O.; Millán, A.; Amaral, V. S.; Palacio, F.; Carlos, L. D. *Nanoscale* **2012**, *4*, 4799.

(2) (a) Cui, Y.; Zhu, F.; Chen, B.; Qian, G. *Chem. Commun.* **2015**, *51*, 7420. (b) McLaurin, E. J.; Bradshwa, L. R.; Gamelin, D. R. *Chem. Mater.* **2013**, *25*, 1283. (c) Wang, X.; Wolfbeis, O. S.; Meier, R. J. *Chem. Soc. Rev.* **2013**, *42*, 7834.

(3) (a) Wu, Y; Liu, J.; Ma, J.; Lin, Y.; Wang, Y.; Wu D. *ACS Appl. Mater. Interfaces* **2016**, *8*, 14396. (b) Albers, A. E.; Chan, E. M.; McBride, P. M.; Ajo-Franklin, C. M.; Cohen, B. E.; Helms, B. A. *J. Am. Chem. Soc.* **2012**, *134*, 9565. (c) Cui, X.; Cheng, Y.; Lin, H.; Huang, F.; Wu, Q.; Wang, Y. *Nanoscale* **2017**, *9*, 13794. (d) McLaurin, E. J.; Bradshaw, L. R.; Gamelin, D. R. *Chem. Mater.* **2013**, *25*, 1283.

(4) (a) Qiao, J.; Wang, Y.-H.; Chen, C.-F.; Qi, L.; Dong, P.; Mu, X.-Y.; Kim, D.-P. *Anal. Chem.* **2015**, *87*, 10535. (b) Ye, F.; Wu, C.; Jin, Y.; Chan, Y.-H.; Zhang, X.; Chiu, D. T. *J. Am. Chem. Soc.* **2011**, *133*, 8146. (c) Zhang, H.; Jiang, J.; Gao, P.; Yang, T.; Zhang, K. Y.; Chen, Z.; Liu, S.; Huang, W.; Zhao, Q. *ACS Appl. Mater. Interfaces* **2018**, *10*, 17542. (temperature-dependent dual fluorescence of polymers)

(5) (a) Cui, Y.; Song, R.; Yu, J.; Liu, M.; Wang, Z. Wu, C.; Yang, Y.; Wang, Z.; Chen, B.; Qian, G. *Adv. Mater.* **2015**, *27*, 1420. (b) Rao, X.; Song, T.; Gao, J.; Cui, Y.; Yang, Y.; Wu, C.; Che, B.; Qian, G. *J. Am. Chem. Soc.* **2013**, *135*, 15559.

(6) (a) Cao, C.; Liu, X.; Qiao, Q.; Zhao, M.; Yin, W.; Mao, D.; Zhang, H.; Xu, Z. *Chem. Commun.* **2014**, *50*, 15811. (b) Zhu, Q.; Yang, W; Zheng, S.; Sung, H. H. Y.; Williams, I. D.; Liu, S.; Tang, B. Z. *J. Mater. Chem. C.* **2016**, *4*, 7383. (c) Chandrasekharan N.; Kelly, L. A. *J. Am. Chem. Soc*. **2001**, *123*, 9898.

(7) Kasha, M. *Discuss. Faraday Soc.* **1950**, *9*, 1420.

(8) (a) Cao, Y.; Nagle, J. K.; Wolf, M. O.; Patrick, B. O. *J. Am. Chem. Soc.* **2015**, *137*, 4888. (b) Cao, Y.; Wang, X.; Shi, X.; Clee, S. M.; McGeer, P. L.; Wolf, M. O.; Orvig, C. *Angew. Chem. Int. Ed.* **2017**, *56*, 15603.

(9) Shi, Y.-G.; Wang, J.-W.; Li, H.; Hu, G.-F.; Li, X.; Mellerup, S. K.; Wang, N.; Peng, T.; Wang, S. *Chem. Sci.* **2018**, *9*, 1902.

(10) Shimogawa, H.; Yoshikawa, O.; Aramaki, Y.; Murata, M; Wakamiya, A.; Murata, Y. *Chem. Eur. J.* **2017**, *23*, 3784.

(11) Zhang, Z.; Wu, Y.-S.; Tang, K.-C.; Chen, C.-L.; Ho, J.-W.; Su, J.; Tian, H.; Chou, P.-T. *J. Am. Chem. Soc.* **2015**, *137*, 8509.

(12) (a) Chen, J.; Wu, Y.; Wang, X.; Yu, Z.; Tian, H.; Yao, J.; Fu, H. *Phys. Chem. Chem. Phys.* **2015**, *17*, 27658. (b) Zhang, Y.; Li, Y.; Wang, H.; Zhang, Z.; Feng, Y.; Tian, Q.; Li, N.; Mei, J.; Su, J.; Tian, H. *ACS Appl. Mater. Interfaces* **2019**, *11*, 39351. (c) Zhang, Z.; Song, W.; Su, J.; Tian, H. *Adv. Funct. Mater.* **2020**, *30*, 1902803. (d) Zhang, Z.; Sun, G.; Chen, W.; Su, J.; Tian, H. *Chem. Sci.* **2020**, *11*, 7525. (e) Song, W.; Ye, W.; Shi, L.; Huang, J.; Zhang, Z.; Mei, J.; Su, J.; Tian, H. *Mater. Horiz.* **2020**, *7*, 615. (f) Liu, H.; Song, W.; Chen, X.; Mei, J.; Zhang, Z.; Su, J. *Mater. Chem. Front.* **2021**, *5*, 2294. (g) Su, Y.; Liu, H.; Chen, X.; Wang, Q.; Su, J.; Zhang, Z. *ACS Appl. Polym. Mater.* **2022**, *4*, 1636. (vibration-induced emission (VIE) molecules)

(13) Shi, L.; Song, W.; Lian, C.; Chen, W.; Mei, J.; Su, J.; Liu, H.; Tian, H. *Adv. Opt. Mater.* **2018**, *6*, 1800190.

(14) (a) Yuan, C.; Saito, S.; Camacho, C.; Irle, S.; Hisaki, I.; Yamaguchi, S. *J. Am. Chem. Soc.* **2013**, *135*, 8842. (b) Yuan, C.; Saito, S.; Camacho, C.; Kowalczyk, T.; Irle, S.; Yamaguchi, S. *Chem. Eur. J.* **2014**, *20*, 2193.

(15) Sk, B.; Khodia, S.; Patra, A. *Chem. Commun.* **2018**, *54*, 1786.

(16) Feng, J.; Tian, K.; Hu, D.; Wang, S.; Li, Y.; Zeng, Y.; Li, Y.; Yang, G. *Angew. Chem. Int. Ed.* **2011**, *50*, 8072.

(17) Fang, Q.; Li, J.; Li, S.; Duan, R.; Wang, S.; Yi, Y.; Guo, X.; Qian, Y.; Huang, W.; Yang, G. *Chem. Commun.* **2017**, *53*, 5702.

(18) (a) Sun, Z. B.; Liu, J. K.; Yuan, D. F.; Zhao, Z. H.; Zhu, X. Z.; Liu, D. H.; Peng, Q.; Zhao, C. H. *Angew. Chem. Int. Ed.* **2019**, *58*, 4840. (b) Liu, D. H.; Sun, Z. B.; Zhao, Z. H.; Peng, Q.; Zhao, C. H. *Chem. Eur. J.* **2019**, *25*, 10179.

(19) (a) Mellerup, S.; Wang, S. *Chem. Soc. Rev.* **2019**, *48*, 3537. (b) Cao, Y.; Wang, X.; Shi, X.; Clee, S. M.; McGeer, P. L.; Wolf, M. O.; Orvig, C. *Angew. Chem. Int. Ed.* **2016**, *55*, 1196. (c) Wang, J.; Wang, N.; Wu, G.; Wang, S.; Li, X. *Angew. Chem. Int. Ed.* **2019**, *58*, 3082. (d) Hou, Q.; Liu, L.; Mellerup, S. K.; Wang, N.; Peng, T.; Chen, P.; Wang, S. *Org. Lett.* **2018**, *20*, 6467. (e) Li, H.-J.; Mellerup, S. K.; Wang, X.; Wang, S. *Org. Lett.* **2019**, *21*, 2838. (f) Matsumoto, T.; Tanaka, K.; Tanaka, T.; Chujo, Y. *Dalton Trans.* **2015**, *44*, 8697. (g) Matsumoto, T.; Takamine, H.; Tanaka, K.; Chujo, Y. *Mater. Chem. Front.* **2017**, *1*, 2368.

(20) (a) Entwistle, C. D.; Marder, T. B. *Angew. Chem., Int. Ed.* **2002**, *41*, 2927. (b) Ji, L.; Griesbeck, S.; Marder, T. B. *Chem. Sci.* **2017**, *8*, 846. (c) Wakamiya, A.; Yamaguchi, S. *Bull. Chem. Soc. Jpn.* **2015,** *88*, 1357. (d) Ren, Y.; Jäkle, F. *Dalton Trans.* **2016**, *45*, 13996. (e) Li, S.-Y.; Sun, Z.-B.; Zhao, C.-H. *Inorg. Chem.* **2017**, *56*, 8705. (f) Mellerup, S. K.; Wang, S. *Chem. Soc. Rev.* **2019**, *48*, 3537.

(21) (a) Malpicci, D. M.; Lucenti, E.; Giannini, C.; Forni, A.; Botta, C. *Molecules* **2021**, *26*, 6999. (b) Demchenko, A. P.; Tomin, V. I.; Chou, P.-T. *Chem. Rev.* **2017**, *117*, 13353. (c) Itoh, T. *Chem. Rev.* **2012**, *112*, 4541.

(22) (a) Lippert, E.; Lüder, W.; Moll, F.; Nägele, W.; Boos, H.; Prigge, H.; Seibold-Blankenstein, I. *Angew. Chem.* **1961**, *73*, 695. (b) Naito, H.; Nishino, K.; Morisaki, Y.; Tanaka, K.; Chujo, Y. *Angew. Chem. Int. Ed.* **2017**, *56*, 254. (c) Ito, A.; Ishizaka, S.; Kitamura, N. *Phys. Chem. Chem. Phys*. **2010**, *12*, 6641. (d) Köhn, A.; Hättig, C. *J. Am. Chem. Soc.* **2004**, *126*, 7399. (e) Choudhury, S. D.; Muralidharan, S.; Pal, H. *Phys. Chem. Chem. Phys*. **2014**, *16*, 11509.

(23) (a) Mahato, P.; Saha, S.; Das, A. *J. Phys. Chem. C* **2012**, *116*, 17448. (b) Sasaki, S.; Drummen, G. P. C.; Konishi, G. *J. Mater. Chem. C* **2016**, *4*, 2731.

(24) (a) Feng, J.; Xiong, L.; Wang, S.; Li, S.; Li, Y.; Yang, G. *Adv. Funct. Mater.* **2013**, *23*, 340. (b) Liu, J.; Guo, X.; Hu, R.; Xu, J.; Wang, S.; Li, S.; Li, Y.; Yang, G. *Anal. Chem.* **2015**, *87*, 3694. (c) Liu, X.; Li, S.; Feng, J.; Li, Y.; Yang, G. *Chem. Commun.* **2014**, *50*, 2778.